Inorganic Chemistry

Article

pubs.acs.org/IC

Aluminum-Stabilized Low-Spin Iron(II) Hydrido Complexes of 1,4,7-Trimethyl-1,4,7-triazacyclononane

Masataka Oishi,[†] Togo Endo,[†] Masato Oshima,[‡] and Hiroharu Suzuki*[,†]

[†]Graduate School of Science and Engineering, Tokyo Institute of Technology, 2-12-1 O-okayama, Meguro-ku, Tokyo 152-8552, Japan

[‡]School of Engineering, Tokyo Polytechnic University, 1583 Iiyama, Atsugi-shi, Kanagawa 243-0297, Japan

Supporting Information

ABSTRACT: We investigated herein the reactions of $(Me_3tacn)FeCl_n$ (**1a**: n = 3, **1b**: n = 2) with common aluminum hydride reagents and a bulky dihydridoaluminate $\{Li(ether)_2\}\{Al(OC_6H_3\text{-}2,6\text{-}^tBu_2)\}(\mu\text{-}H)_2$, which yielded the diamagnetic hydrido complexes **2**−**4** containing Fe(II) and Al(III). In particular, the use of divalent **1b** afforded excellent isolated yields. The structures of **2**−**4** were determined using spectroscopic and crystallographic analyses. The crystal structures showed distorted octahedral Fe centers and fairly short Fe−Al distances [2.19−2.24 Å]. The structures of cation moiety **2** and neutral complex **4** were further probed using DFT calculations, which indicated a stable low-spin Fe(II) state and strongly electron-donating nature of the $(Me_3tacn)FeH_3$ fragment toward the Al(III) center.

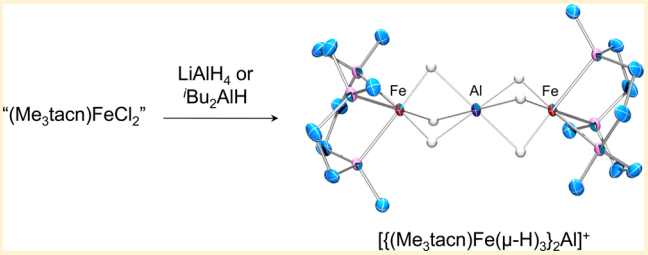

INTRODUCTION

Dinuclear transition metal motifs are found as the active centers of a number of metalloenzymes,[1] wherein the transition metal centers are typically stabilized by the amino acid residues of polypeptides and siderophores. Successful models of hemeerythrin as an oxygen-storage metalloprotein have been described as O-bridged diiron frameworks supported by the facial nitrogen-based ligands 1,4,7-triazacyclononanes (tacn)[2] and hydrotris(pyrazolyl)borates (Tp).[3]

Despite these pioneering studies on the di-iron oxo complexes, little known are the corresponding hydrido forms having these ligand systems. Hitherto, the syntheses of the related dinuclear hydrido clusters of group 8 and 9 metals by Wieghardt,[4] our group,[5] Paneque, and Ruiz,[6] respectively, have involved $[(Me_3tacn)_2Rh_2(H)_2(\mu\text{-}H)_2]^{2+}$, $[(Me_3tacn)_2M_2(\mu\text{-}H)_3]^+$ (M = Fe, Ru), and $[(Tp^{Me_2})_2Ir_2(H)_2(\mu\text{-}H)(\mu\text{-}L)]$ (L = Cl, SC_4H_3). We became intrigued with their reactivity toward unactivated substrates, compared to other ligand systems of Cp, CO, and triphos. Additionally, the formation of heterobinuclear complexes implies anisotropic reactivity.[7] For instance, a recent study from our laboratory has shown promising reactivity of the diruthenium hydride containing a $(Me_3tacn)Ru$ unit, $\{(Me_3tacn)Ru\}(Cp^*Ru)(\mu\text{-}H)_3$, with CO_2 (1 atm), leading to the formation of the bis(μ-formato) complex, whereas $(Cp^*Ru)_2(\mu\text{-}H)_4$ exhibited no reactivity even at a much higher pressure of CO_2.[7b] The development of useful starting (hydrido) complexes is crucial before the initiation of systematic reactivity studies. We report herein the reactions between Me_3tacn-ligated iron(II) and -(III) chlorides and several hydride reagents and the structures of the iron(II) hydrido complexes.

RESULTS AND DISCUSSION

1. Reaction of $(Me_3tacn)FeCl_3$ (1a) and $LiAlH_4$. Primarily, we reinvestigated the reaction of $(Me_3tacn)FeCl_3$ (**1a**) with $LiAlH_4$ using Wieghardt's procedure (Scheme 1).[4]

Scheme 1

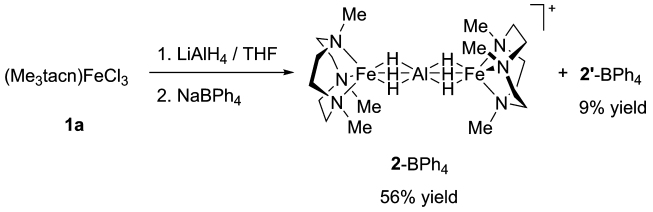

After counteranion exchange with $NaBPh_4$, a THF-soluble fraction was separated from the reaction mixture, and two signals in the hydrido region of the ^1H NMR spectrum (THF-d_8, rt) were observed at δ −24.1 and −25.7 ppm with an integration ratio of 6:1 (56% and 9% NMR yields, respectively). The chemical shift of the former major resonance was close to that reported previously.[4] The major component (**2**-BPh_4) was isolated as purple platelets by recrystallization from THF. The reddish-purple platelet crystals of the minor product **2′**-BPh_4 were eventually obtained from a THF/toluene mixture. The preliminary X-ray analysis of the sample suggested that **2′**-BPh_4 might be a monocation having two Fe−H_3−Al fragments,[8] which was analogous to the structure of **3** (shown later). The

Received: January 27, 2014
Published: May 6, 2014

   dx.doi.org/10.1021/ic500195q | Inorg. Chem. 2014, 53, 5100−5108

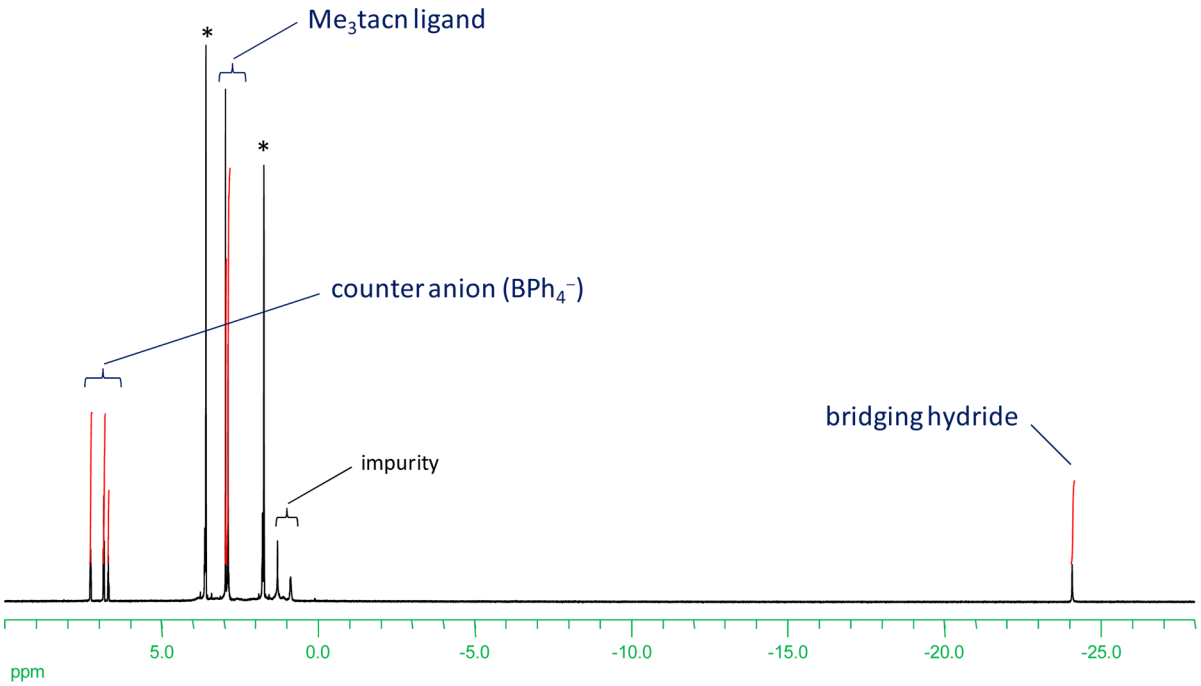

Figure 1. ^{1}H NMR spectrum of **2**-BPh_4 (THF-d_8). Asterisks denote solvent.

structure of **2**-BPh_4 was established using NMR and single-crystal X-ray analyses. As reported previously, this material was highly air- and moisture-sensitive and immediately decolorized on exposure to air and moisture.[4] Once purified, **2**-BPh_4 became decreasingly soluble in THF to a great extent. The ^{1}H NMR spectrum of the pure, diamagnetic **2**-BPh_4 clearly showed resonances of Me_3tacn and counteranion moieties as well as a single hydride resonance (Figure 1). The spectrum of **2**-BPh_4, however, showed two $(Me_3tacn)Fe(H)_3$ fragments over one counteranion based on the integration ratio of the tacn ligand, hydride, and borate.

Moreover, the X-ray analysis of **2**-BPh_4 unequivocally demonstrated a structure with two iron fragments and one borate, in accordance with the ^{1}H NMR data. As shown in Figure 2, the crystal structure of **2**-BPh_4 has a linear three-metal-centered core, Fe−Al−Fe [Fe1−Al1−Fe1# = 180°]. In the solid-state structure, each of the two Me_3tacn−Fe fragments of **2**-BPh_4 adopted $\delta\delta\delta$ and $\lambda\lambda\lambda$ tacn configuration, respectively. The Fe−Al distances [2.1918(5) and 2.1879(4) Å] were significantly shorter than the distances of known Fe−Al bonds.[9] Fischer and co-workers reported $FeAl_4$ and $FeAl_5$ hydrido clusters, in which unsupported Fe−Al bonds [2.21−2.26 Å] were shorter than the hydride-bridged Fe−Al bonds [2.32−2.44 Å].[9b] However, in the crystal structure of **2**-BPh_4 three bridging hydride ligands were located between Fe and Al atoms in the difference Fourier map, and the hydride-bridged Fe−Al distance of **2**-BPh_4 was shorter than those in the above examples as well as unsupported Fe−Al-bonded complexes.[10] In addition, an ^{27}Al{^{1}H} NMR spectrum of **2**-BPh_4 (THF-d_8, 60 °C) demonstrated the presence of the aluminum atom, whose resonance was observed at δ 97.9 ppm with a relatively smaller half-height width ($w_{1/2}$) of 79 Hz. The resultant ^{27}Al NMR parameters were reasonable for the highly symmetric aluminum hydrides.[11]

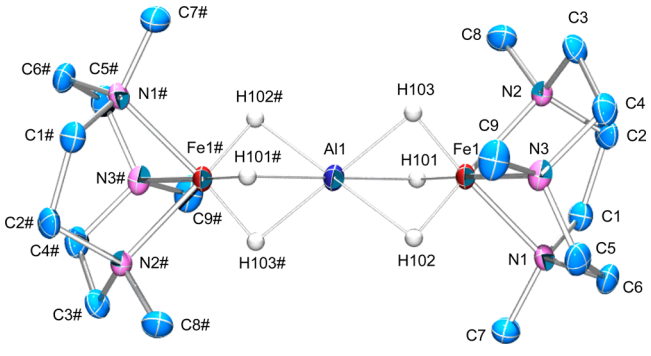

Figure 2. Crystal structure of $[\{(Me_3tacn)Fe(\mu\text{-}H)_3\}_2Al]BPh_4$ (**2**-BPh_4) (cation structure of one of the two independent molecules). Hydrogen atoms in Me_3tacn ligands are omitted for clarity. Thermal ellipsoids are drawn at the 50% probability level. Selected bond distances (Å) and angles (deg): Fe1−Al1 2.1918(5), Fe1−N1 2.043(3), Fe1−N2 2.040(3), Fe1−N3 2.031(3); Fe1−Al1−Fe1 180.0; Fe2−Al2 2.1879(4), Fe2−N4 2.040(3), Fe2−N5 2.035(3), Fe2−N6 2.035(3); Fe2−Al2−Fe2 180.0.

In order to obtain insight into the Fe−H_3−Al structure, we performed DFT calculation of **2** at the B3LYP level of theory. The optimized structure of cation **2** (singlet state) and selected bond distances of the singlet and triplet states are shown in Figure 3 and Table 1, respectively. The geometrical parameters of the singlet state agreed with those obtained from the X-ray analysis, in particular, in terms of Fe−Al and Fe−N distances [2.222 and 2.059 Å, respectively]. However, the corresponding triplet state indicated a relatively low symmetrical structure of the two $(Me_3tacn)Fe$ fragments. Subsequently, the calculation indicated that the triplet state of **2** was much higher in energy compared to the corresponding singlet state; that is, the free energy difference between the two states was estimated to be 17.9 kcal mol^{-1} (Table S1).

Although the molecular orbitals of singlet-state **2** were somewhat complicated, six occupied high-lying HOMO to HOMO−5 and six unoccupied molecular orbitals LUMO+2, +3, +7, +8, +10, and +11 were found to have major

dx.doi.org/10.1021/ic500195q | Inorg. Chem. 2014, 53, 5100−5108

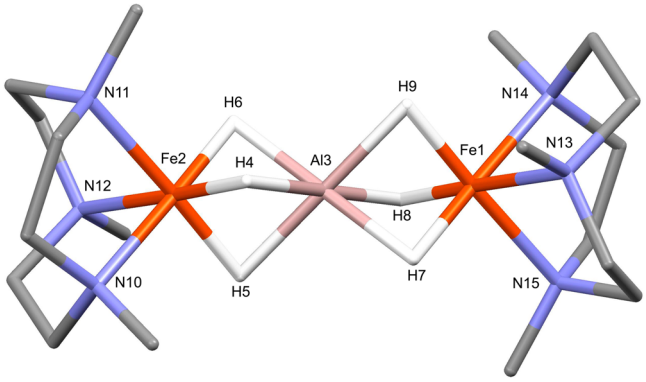

Figure 3. DFT-optimized structures of **2** (singlet state).

Table 1. Selected Bond Distances (Å) from DFT-Optimized and Experimentally Determined Structures of 2

	DFT		X-ray	
bond	singlet state	triplet state	2-BPh_4	2-$^i Bu_2AlCl_2$
Fe1−Al3	2.2220	2.2233	2.1918(5) 2.1879(4)	2.1906(3)
Fe2−Al3	2.2220	2.3178		
Fe1−N(av)	2.0590	2.0610	2.038 2.038	2.042
Fe2−N(av)	2.0590	2.1423		
Fe1−H(av)	1.6478	1.6454	1.44 1.56	1.55
Fe2−H(av)	1.6577	1.7487		

contributions from Fe-based d orbitals (Figure S1-1). Clear N−Fe−H bonding orbital interactions were found in fairly low-lying HOMO−11, −12, −14, and −15 (Figure 4), whereas occupied molecular orbitals were not clearly found, implying the presence of either Al−H or Al−Fe bonding interaction. As listed in Table 2, the NBO analysis indicated the presence of

Table 2. NBO Analysis of Optimized 2

	natural charge	bond	Wiberg index
Fe (av)	+0.0419	Fe−H	0.4726−0.4738
Al	+1.0801	Fe−N	0.2518−0.2526
N (av)	−0.4740	Fe−Al	0.2764
μ-H (av)	−0.2210	Al−H	0.3662−0.3676
Me_3tacn	+0.5811		

positively charged Al (+1.08) and negatively charged N (−0.47) and H (−0.22) centers with a higher covalent bond order for Fe−H (0.47) than that for Fe−Al (0.28). The relatively small covalent bond indexes for Fe−H and Fe−N could be ascribed to contributions from Fe−H antibonding orbital interactions found in HOMO−35, −16, −10, and −9 and from Fe−N antibonding orbital interactions found in HOMO−13, −10, −9 to −7, and −6 (Figures S1, S2). Although the covalent bond index for each Al−H (0.37) is small, the sum of the bond indexes for the three Al−H (total 1.10) may indicate the presence of sufficient bonding interaction between the Al and the almost electrically neutral (Me_3tacn)FeH_3 moiety (total charge −0.040). Previous reports on crystallographically characterized transition metal−aluminum complexes with triply bridging hydrides are limited to Re−Al, W−Al, and Sc−Al hydrides.[12] The formal shortness ratios (FSRs)[13] for the metal−aluminum distance in these complexes are in a range of 0.99−1.03. In contrast, **2**-BPh_4 has a smaller

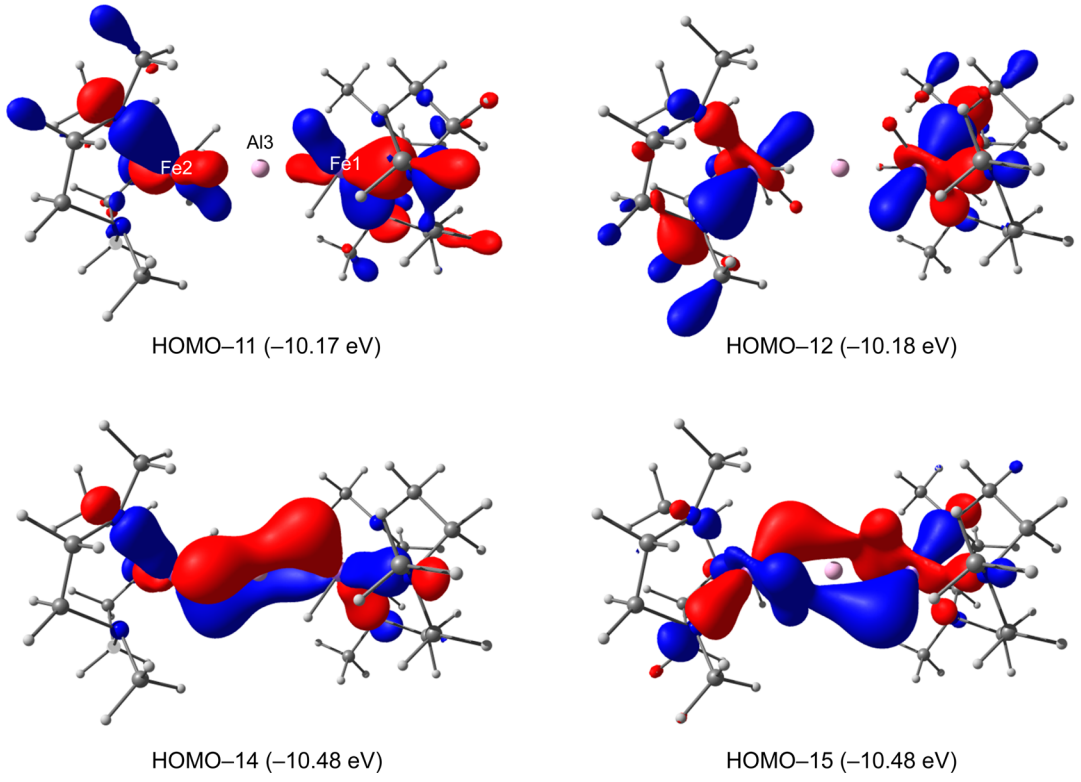

Figure 4. Molecular orbitals (HOMO−11, −12, −14, and −15) in **2** including N−Fe−H bonding interactions. Each orbital is drawn by a 0.04 contour value.

dx.doi.org/10.1021/ic500195q | *Inorg. Chem.* 2014, 53, 5100−5108

FSR (0.91). This may be due to the presence of Fe and Me_3tacn as the electron-rich late metal and ligand. Therefore, we concluded that the experimentally observed short Fe−Al distance resulted from the strong donating property of the polarized $(Me_3tacn)FeH_3$ fragments toward the Al(III) center. Such a Fe_2AlH_6 core structure with any ligand systems has not been reported hitherto; rather experimental and theoretical studies on the structures of Fe_2BH_6, $[\{(R_3P)_3Fe\}_2B(\mu\text{-}H)_6]^+$ (R = Et, R_3 = triphos), have been reported.[14] The bonding nature of D_{3d}-symmetric Fe_2BH_6 was interpreted as having direct Fe−B bonds and a hypervalent boron center.

2. Reactions of $(Me_3tacn)FeCl_2$ (1b) and Other Hydride Reagents. The structure and iron formal oxidation state of **2**-BPh_4 led us to examine the reactions of the corresponding Fe(II) chloride as a starting complex with other known hydride reagents. $(Me_3tacn)FeCl_2$ (**1b**), reported by Rauchfuss and his co-worker, is composed of a dinuclear cation and mononuclear anion $[\{Me_3tacn)Fe\}_2(\mu\text{-}Cl)_3][(Me_3tacn)FeCl_3]$ (described as "$(Me_3tacn)FeCl_2$" for simplicity).[15] **1b** was suspended in THF and treated with 5 equiv of DIBAL-H at 25 °C to yield a purple solution (Scheme 2). After workup, a viscous solid was

Scheme 2. Reaction of 1b with Either DIBAL-H or $LiAlH_4$

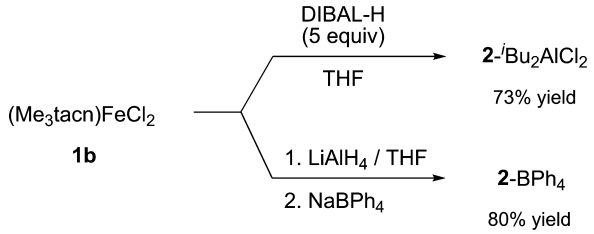

obtained. The ^1H NMR spectrum in C_6D_6 showed that the product, having a characteristic hydride resonance at δ −24.0 ppm, resembled **2**-BPh_4 except for the resonances of the counteranion moiety. The recrystallization of the product from a THF/pentane mixture at ambient temperature yielded purple platelets, which allowed us to carry out single-crystal X-ray studies. The results of both X-ray and NMR studies were consistent with the formulation of **2**-^{i}Bu_2AlCl_2 (see CIF file). The S_6-symmetric cation was essentially the same as that in **2**-BPh_4. Cations **2** were reproducibly formed from **1b** with either DIBAL-H or $LiAlH_4$ with over 70% isolated yields, which were much higher and more selective than those from the trivalent iron chloride **1a** (Scheme 2).

A reaction of **1a** with DIBAL-H was also performed, yielding **2**-^{i}Bu_2AlCl_2 along with a minor product, which showed a hydride resonance at −25.1 ppm in the ^1H NMR spectrum (hydride integration ratio: **2**-^{i}Bu_2AlCl_2/the minor product = 3.2:1). The structure of the minor product was tentatively assigned to **2′**-^{i}Bu_2AlCl_2.

We also reacted **1b** with borohydride reagents such as $LiBH_4$, $LiEt_3BH$, and $NaBH_4$ under similar conditions; however, all attempts resulted in the formation of paramagnetic black solids. These materials were insoluble in THF, CH_3CN, and CH_2Cl_2 and reacted with protic solvents. This led to the evolution of gas; therefore, we did not characterize them any further. Next, we turned our attention to the use of another aluminum-based hydride reagent, $NaAlH_2(OCH_2CH_2OMe)_2$ (Red-Al). When 5 equiv of Red-Al was employed for **1b** in THF, the reaction proceeded at 25 °C and reached completion in 24 h, affording the diamagnetic purple product **3** (Scheme 3). **3** was soluble in

Scheme 3

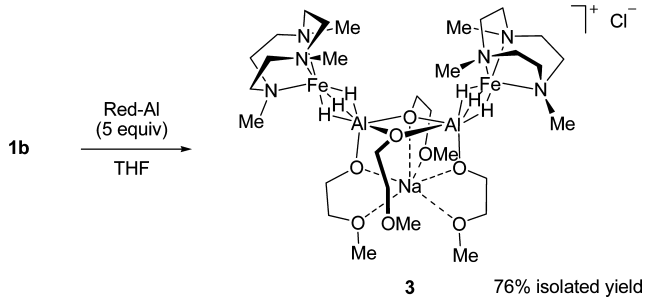

THF but insoluble in pentane, toluene, and ether. It was readily isolated as red-purple platelets after filtration and recrystallization from a THF/ether mixture (76% isolated yield based on **1b**). ^1H NMR and COSY spectra of **3** (THF-d_8) exhibited not only the characteristic resonances of Me_3tacn ligand protons (δ 2.95 and 2.93−3.06 ppm for Me and CH_2CH_2, respectively) and hydride (δ −25.6 ppm) but also proton signals of the 2-methoxyethoxy group in the typical magnetic field (δ 3.41 and 3.43−3.92 ppm for Me and CH_2CH_2, respectively). $T_{1\ min}$ for the hydride signal was measured [130(1) ms at 235 K]. The value indicates the absence of the nonclassical hydride nature of **3**.[16]

The X-ray analysis of **3** was performed, and the molecular structure is presented in Figure 5. The solid-state structure of **3**

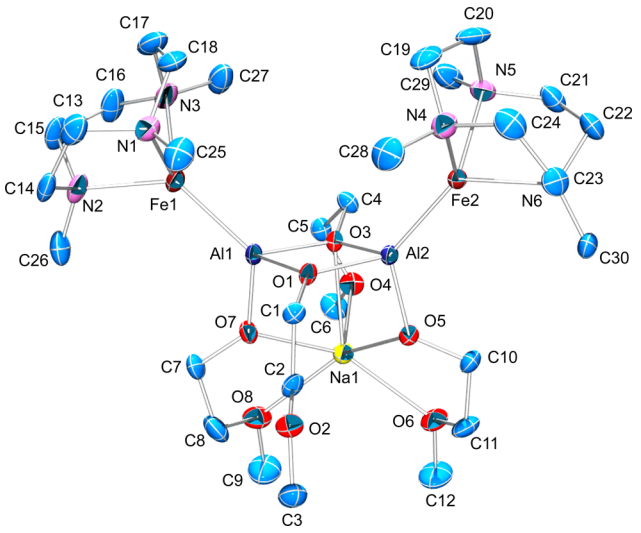

Figure 5. Crystal structure of **3** (cation moiety only). Hydride ligands could not be located. All other hydrogen atoms are omitted for clarity. Thermal ellipsoids are drawn at the 50% probability level. Selected bond distances (Å) and angles (deg): Fe1−Al1 2.2450(17), Fe1−N1 2.064(5), Fe1−N2 2.072(5), Fe1−N3 2.044(5), Al1−O1 1.860(4), Al1−O3 1.891(4), Al1−O7 1.780(4); O1−Al1−O3 79.05(15), O3−Al1−O7 92.25(18), O1−Al1−O7 97.47(18).

showed two Fe−Al units linked by alkoxyl ligands on the Al atoms and one Na atom trapped by six alkoxide and ethereal oxygen atoms. The Fe−Al distance [Fe1−Al1 = 2.2450(17) Å] was comparable to that of **2**. The incorporation of the Na and Cl atoms into the molecule apparently decreased the solubility of the complex in organic solvents and resulted in a *syn* configuration of the Fe1−Al1−Al2−Fe2 core. We attempted to liberate the Na cation in the structure of **3** by addition of excess

dx.doi.org/10.1021/ic500195q | Inorg. Chem. 2014, 53, 5100−5108

crown ethers (15-crown-5 and 18-crown-6). However, NaCl elimination did not occur even at elevated temperatures.

Lithium and sodium aluminum dihydrides bearing bulky aryloxides were reported by Nöth and co-workers.[17] We envisaged that the lithium hydridoaluminate $\{Li(OEt_2)_2\}\{Al(ArO)_2\}(\mu\text{-}H)_2$ (Ar = C_6H_3-2,6-^{t}Bu$_2$) would serve as a hydride reagent to afford a neutral Fe−H_3−Al complex, into which a lithium salt (byproduct) would no longer be incorporated owing to the presence of the sterically congested $Al(OAr)_2$ moiety. The reaction of **1b** with 5 equiv of $\{Li(OEt_2)_2\}\{Al(ArO)_2\}(\mu\text{-}H)_2$ in THF led to the formation of Fe−Al hydride **4** (Scheme 4). **4** was readily isolated by the filtration of

Scheme 4

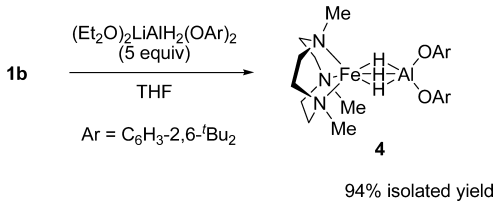

insoluble byproducts followed by the evaporation of THF solvent and successive removal of the remaining aluminum hydride reagent by simply rinsing the residue with ether and a small amount of toluene. This was because **4** was moderately soluble in THF but scarcely soluble in ether and toluene. The structure of **4** was established using spectroscopy and crystallography. The ^{1}H NMR spectrum recorded at 25 °C displayed a characteristic resonance at δ −25.20 ppm for the three hydrides, which were observed to be equivalent at the temperature. Consequently, the signals of two aryloxide ligands on aluminum as well as methyl proton signals of Me_3tacn on iron were also observed to be equivalent on the NMR time scale. The single crystals of **4**, suitable for X-ray analysis, were grown by the slow diffusion of ether into the THF solution. The crystal structure of **4** is shown in Figure 6. The structure of the distorted octahedral iron hydride moiety and intermetal distance [Fe1−Al1 = 2.2137(4) Å] in **4** were essentially the same as those in the complexes **2** and **3**. One exception was the pentacoordinated Al center, in which the four atoms Fe1, Al1, O1, and O2 share the same plane: summation of aluminum angles = 360.0° [O1−Al1−O2 = 96.05(5)°, O1−Al1−Fe1 = 134.42(4)°, O2−Al1−Fe1 = 129.54(4)°].

The DFT calculation of the neutral complex **4** (singlet state) was also carried out. As summarized in Table S5, the DFT-optimized structure of **4** is in good agreement with the crystal structure in terms of Fe−Al, Fe−N, and Al−O distances and O−Al−O angle (within 3% error). The molecular orbital diagrams of **4**, presented in Figure S2-1 and S2-2, are more comprehensive than those of **2**. The Fe-based nonbonding orbitals were clearly found in the three molecular orbitals HOMO, HOMO−1, and HOMO−2. Fe−N and Fe−H bonding interactions were mainly observed in the low-lying HOMO−12 and −13, whereas the LUMO+5, +6, and +7 displayed antibonding orbital interactions of Fe−N, Fe−H, and Fe−Al (Figure S2-1). The NBO analysis of **4**, summarized in Table S6, showed nearly identical bonding interactions in the $(Me_3tacn)FeH_3Al$ moiety with those in cation **2** (natural charge in **4**: Fe −0.0421, Al +1.7106, N_{av} −0.4857, and Me_3tacn +0.5131; Wiberg index in **4**: Fe−Al 0.2164, Fe−H 0.4916−0.5950, Al−H 0.2214−0.3005).

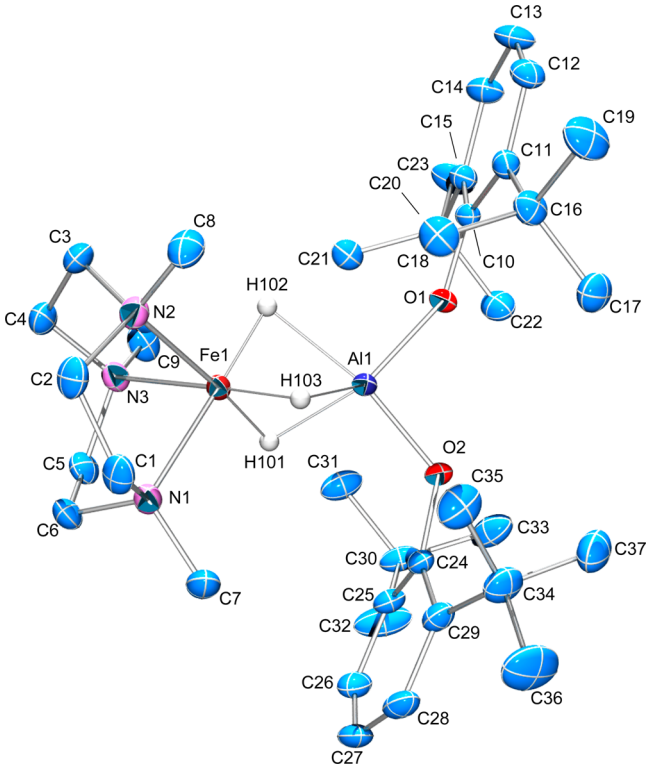

Figure 6. Crystal structure of **4**. Hydrogen atoms in Me_3tacn, alkoxide ligands, and a crystallization THF solvent are omitted for clarity. Thermal ellipsoids are drawn at the 50% probability level. Selected bond distances (Å) and angles (deg): Fe1−Al1 2.2137(4), Fe1−N1 2.0622(12), Fe1−N2 2.0610(12), Fe1−N3 2.0439(12), Al1−O1 1.7444(10), Al1−O2 1.7817(10); N1−Fe1−N2 84.17(5), N2−Fe1−N3 84.48(5), N1−Fe1−N3 84.59(5), O1−Al1−O2 96.05(5).

3. Electronic Spectra of Fe(II) Hydrides. To verify the preference of the low-spin Fe(II) center, UV−vis spectra of diamagnetic **2**−**4** were recorded (Figure 7). The detected absorption bands in the spectra of **2**−**4** are listed in Table 3 for comparison with those of related low-spin Fe(II) complexes. In contrast to nearly colorless Fe(II) complexes **1b** and $[\{(Me_3tacn)Fe\}_2(\mu\text{-}Cl)_3]BPh_4$,[14,18d] **2**-$BPh_4$ and **2**-^{t}Bu$_2$$AlCl_2$, having common cationic structure, yielded almost identical absorptions in both the UV and visible-light regions. The spectra include four bands, two of which (**2**-BPh_4: 543 and 311 nm; **2**-^{t}Bu$_2$$AlCl_2$: 537 and 328 nm) were assignable to typical spin-allowed d−d transitions of low-spin Fe(II) complexes.[14] As mentioned above in the DFT results, owing to the large energy difference between the two spin states, there was no contribution from the high-spin Fe(II) electronic configuration to the spectra. These characteristic bands for low-spin Fe(II) states were also detected in the spectra of **3** and **4**; however, the two extra bands corresponding to ∼455 and ∼390 nm detected in the spectra of **2** were not clearly observed for **3** and **4**. Interestingly, the two common absorption bands of **2**−**4** (522−543 and 310−360 nm) were significantly blue-shifted and had much higher molar extinction coefficients than those of previously reported low-spin Fe(II) (Table 3).

CONCLUSIONS

The synthesis of Al-capped $(Me_3tacn)FeH_3$ complexes **2**−**4** was accomplished through the reaction of **1** with aluminum-based hydride reagents under mild conditions, irrespective of the valency of the starting iron chlorides. On the other hand,

dx.doi.org/10.1021/ic500195q | Inorg. Chem. 2014, 53, 5100−5108

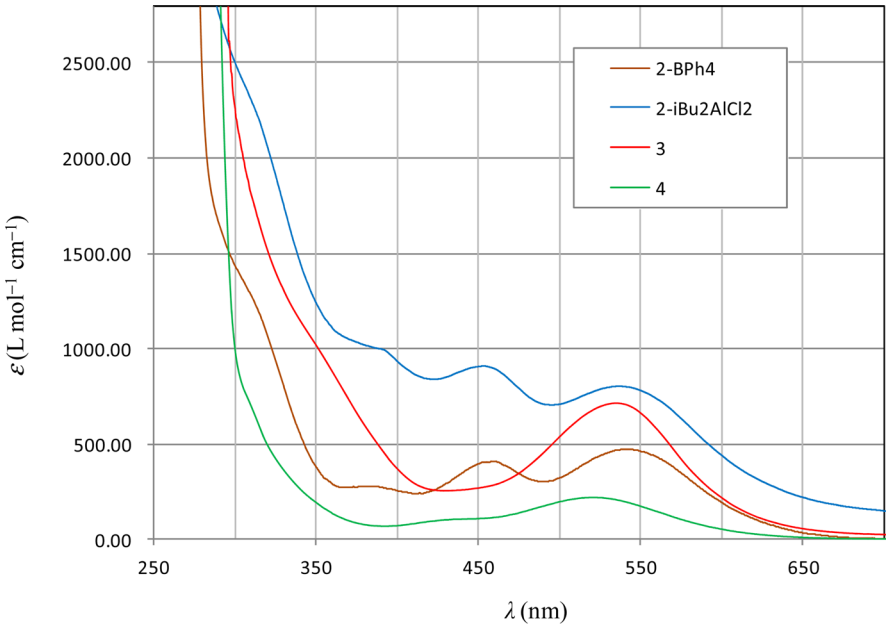

Figure 7. UV−vis spectra of **2**−**4** (0.24−1.70 mM in THF at 25 °C).

Table 3. Comparison of Electronic Transitions of Fe(II) Complexes

complex	solvent	λ, nm (ε, L mol^{-1} cm^{-1})	ref
$[Fe(tacn)_2]Br_2$	H_2O	601 (6), 387 (17), 288 (560)	18b
$[Fe(Me_3tacn)(NCMe)_3](OTf)_2$	MeCN	562 (23), 388 (43)	18d
$[Fe(Me_3tacn)(NCMe)_3](BPh_4)_2$	MeCN	577 (40), 384 (58)	18d
[Fe(*trans*-diammac)]$(PF_6)_2$[a]	D_2O	584 (100), 405 (140)	18e
[Fe{$(NH_2)_2$sar}]$(OTf)_2$[b]	D_2O[c]	590 (14), 394 (15)	18f
2-BPh_4	THF	**543** (452), 457 (412), 388 (295), **311** (1180)[d]	this work
2-$^i Bu_2AlCl_2$	THF	**537** (800), 454 (907), 391 (990), **328** (1810)[d]	this work
3	THF	**535** (716), **360** (878)[d]	this work
4	THF	**522** (208), **310** (827)[d], 282 (4461)[e]	this work

[a]diammac = *exo*-6,13-diamino-6,13-dimethyl-1,4,8,11-tetraazatetradecane. [b]$(NH_2)_2$sar = 1,8-diamino-3,6,10,13,16,19-hexaazabicyclo[6.6.6]-eicosane. [c]pH = 8.5. [d]Observed as a shoulder. [e]Assigned to an absorption of aryloxy group by comparison with the spectrum of $\{Li(OEt_2)_2\}\{Al(ArO)_2\}(\mu\text{-}H)_2$ (Ar = 2,6-di-*tert*-butylphenyl).

commonly used borohydrides, such as $NaBH_4$ and $LiEt_3BH$, yielded only insoluble unidentified materials. The X-ray analysis of **2**−**4** clearly revealed significantly short Fe−Al distances (ca. 2.2 Å). The trihydride-bridged Fe−Al structures were probed using DFT calculations for **2** and **4**, which suggested a stable low-spin Fe(II) state and the presence of a strongly electron-donating property of the polarized $[(Me_3tacn)Fe(\mu\text{-}H)_3]$ and the Lewis acidic Al(III) center. The UV−vis spectra of **2**−**4** included the characteristic absorption bands for low-spin Fe(II) species with a significant blue shift of the LF transitions. These spectroscopic features agreed with the diamagnetic nature, as revealed from the NMR and DFT analysis. Hagen reported the temperature-dependent spin-crossover behavior of $[(Me_3tacn)FeL_3]^{2+}$ (L = acetonitrile and trifluoromethanesulfonate), where the subtle structural change, i.e., the type of L and N-substituents (^{i}Pr and ^{i}Bu) in the tacn ligand, dramatically altered the spin states.[19] We conclude that the low-spin Fe(II) state in **2**−**4** was governed by the presence of the hydride ligands as σ-donors. Moreover, at the same time, the Al fragment played an important role in stabilizing the polarized $[(Me_3tacn)Fe(\mu\text{-}H)_3]$ fragment. So far, several bimetallic hydrides of Fe(II) and main group metals (e.g., B, Si, Sn) with other facial ligand systems, e.g., triphos, have been synthesized and structurally characterized.[20] The synthetic application of the Fe−H_3−Al species to other heterobimetallic hydrides is currently under investigation in our laboratory.

EXPERIMENTAL SECTION

General Procedures. All manipulations for air- and moisture-sensitive compounds were carried out under an argon atmosphere using standard Schlenk techniques or in a glovebox filled with argon (H_2O < 1 ppm, O_2 < 1 ppm). Dehydrated solvents (toluene, pentane, ether, tetrahydrofuran, acetonitrile, methylene chloride, and methanol) were purchased from Kanto Chemical Co. Ltd. Deuterated solvents (benzene-d_6, tetrahydrofuran-d_8, and toluene-d_8) were purchased from Cambridge Isotope Laboratories, Inc. and Sigma-Aldrich Co. (Non)-deuterated hydrocarbon and ethereal solvents were distilled from Na−K alloy and stored under an argon atmosphere. Other reagents and organic and inorganic chemicals were used as received.

Instrumentation. ^{1}H and ^{13}C NMR spectra were recorded on Varian INOVA 400 and Varian 400-MR Fourier transform spectrometers. ^{1}H chemical shifts were referenced to the residual proton peaks of benzene-d_6 at δ 7.15 ppm or tetrahydrofuran-d_8 at δ 3.58 ppm vs tetramethylsilane at δ 0.00 ppm. NMR yields were estimated by integration changes based on integrations of 2,2,4,4-tetramethylpentane as an internal standard. The central peak of a triplet for benzene-d_6 at δ 128.0 ppm or the central peak of a quintet for tetrahydrofuran-d_8 at δ 67.57 ppm vs tetramethylsilane δ 0.00 ppm was used as the ^{13}C NMR internal reference. The peak for $Al(NO_3)_3$ (D_2O) was used as an ^{27}Al NMR external reference. UV−vis spectra were recorded on a Shimadzu UV-2550 spectrophotometer. Infrared spectra were recorded on a JASCO FT-IR 4200 type A spectrophotometer. Elemental analyses (C, H, and N) were recorded on a PerkinElmer 2400II. Single crystals suitable for X-ray analysis were coated with Paratone-N in a glovebox. Crystals of proper size were picked by using a nylon CryoLoop and quickly transferred in a low-temperature N_2 stream to the goniometer head. The diffraction

dx.doi.org/10.1021/ic500195q | Inorg. Chem. 2014, 53, 5100−5108

Table 4. Crystallographic Data of 2-BPh_4, 2-^{i}Bu$_2$AlCl$_2$, 3, and 4

complex	2-BPh_4	2-^{i}Bu$_2$AlCl$_2$	3	4
empirical formula	$C_{42}H_{68}AlBFe_2N_6$	$C_{26}H_{66}Al_2Cl_2Fe_2N_6$	$C_{30}H_{76}Al_2ClFe_2N_6NaO_8$	$C_{41}H_{74}AlFeN_3O_3$
mol wt (g mol^{-1})	800.47	699.41	873.07	739.86
cryst habit	platelet	platelet	platelet	block
cryst syst	monoclinic	monoclinic	monoclinic	monoclinic
space group	$P2_1/a$ (#14)	$C2/c$ (#15)	$P2_1/n$ (#14)	$P2_1/n$ (#14)
cryst color	red	red	red	red
cryst size (mm)	0.15 × 0.07 × 0.05	0.54 × 0.13 × 0.05	0.39 × 0.37 × 0.10	0.51 × 0.28 × 0.23
a (Å)	16.0332(8)	12.3874(7)	15.5885(5)	10.1258(2)
b (Å)	15.8365(8)	11.9798(7)	17.5040(5)	16.6997(4)
c (Å)	17.3741(9)	25.1828(15)	16.9997(5)	24.9425(6)
α (deg)				
β (deg)	100.921(2)	92.973(2)	97.035(3)	90.111(1)
γ (deg)				
V (Å^3)	4331.6(4)	3732.1(4)	4603.6(2)	4217.7(2)
Z value	4	4	4	4
measurement temp (°C)	−150	−150	−150	−150
D_{calc}(g cm^{-3})	1.237	1.245	1.261	1.165
μ(Mo Kα) (mm^{-1})	0.725	0.992	0.781	0.417
$2\theta_{max}$ (deg)	55	51	51	55
reflns collected	35 022	15 313	74 772	68 315
indept reflns	9849 (R_{int} = 0.0918)	3606 (R_{int} = 0.0411)	14417 (R_{int} = 0.0795)	9645 (R_{int} = 0.0324)
reflns obsd (>2σ)	6177	3062	10 526	8491
abs corr type	empirical	empirical	empirical	numerical
abs transmn	0.6907 (min.)	0.4513 (min.)	0.5516 (min.)	0.8258 (min.)
	1.0000 (max.)	1.0000 (max.)	1.0000 (max.)	1.0000 (max.)
R_1 ($I > 2\sigma(I)$)	0.0509	0.0356	0.0822	0.0344
R_1 (all data)	0.1019	0.0403	0.1120	0.0401
wR_2 (all data)	0.1206	0.0865	0.2477	0.0935
data/restraints/params	9849/0/492	3429/0/193	14 417/0/462	9645/0/672
goodness of fit on F^2	1.058	1.057	1.064	1.039
largest diff peak	0.688	0.849	1.92	0.761
and hole (e Å^{-3})	−0.842	−0.318	−1.90	−0.628

data were collected on a R-AXIS RAPID diffractometer equipped with graphite-monochromated Mo Kα radiation (λ = 0.71069 Å). Structures were solved by heavy-atom Patterson or direct methods and expanded using Fourier techniques. The non-hydrogen atoms were refined by full-matrix least-squares refinement in F^2 using the SHELXS-97 program.[21] The twin refinement of complex **3** was performed with SHELXS using the data in HKLF5 format. Hydrogen atoms were located by difference Fourier maps and refined isotropically. Crystallographic data of 2-BPh_4, 2-^{i}Bu$_2$AlCl$_2$, **3**, and **4** are summarized in Table 4.

Synthesis of 2-BPh_4. To a suspension of **1b** (0.106 mmol, 95 mg) in THF (6 mL) was added $LiAlH_4$ (2.03 mmol, 77 mg) at 25 °C under an argon atmosphere. After the mixture was stirred at this temperature for 1.5 h while the reaction system was closed, $NaBPh_4$ (0.16 mmol, 55 mg) was subsequently added under argon purge. After stirring for 24 h, the resulting purple suspension was filtered through glass frits and the insoluble salts were washed with THF (0.5 mL × 2). Solvent was removed from the combined filtrates under reduced pressure, and then the residue was washed with ether to afford essentially pure 2-BPh_4 (102 mg, 80%). Storage of a concentrated THF solution of 2-BPh_4 at −30 °C afforded diffraction quality crystals. ^{1}H NMR (THF-d_8, rt): δ 7.26 (8H, m, Ph-H, *ortho*), 6.84 (8H, t, J = 6.8 Hz, Ph-H, *meta*), 6.69 (4H, t, J = 6.8 Hz, Ph-H, *para*), 2.95 (18H, s, NMe), 2.87 (24H, m, NCH_2), −24.1 (6H, s, μ-H) ppm. ^{13}C{^{1}H} NMR (THF-d_8, rt): δ 164.7 (q, J_{BC} = 49.1 Hz, Ph-*ipso*), 136.7 (Ph-*ortho*), 125.2 (Ph-*meta*), 121.4 (Ph-*para*), 60.2 (NCH_2), 59.3 (NCH_3) ppm. ^{27}Al{^{1}H} NMR (THF-d_8, 60 °C): δ 97.9 ppm ($w_{1/2}$ = 79 Hz). IR (KBr, cm^{-1}): ν 2897 (m), 1655 (s), 1578 (s), 1457 (s), 1289 (m), 1078 (m), 1011 (s), 732 (s), 706 (s), 612 (s). Anal. Calcd for $C_{42}H_{68}AlBFe_2N_6$: C, 62.55; H, 8.50; N, 10.42. Found: C, 62.36; H, 9.00; N, 10.47.

Synthesis of 2-^{i}Bu$_2$AlCl$_2$. To a suspension of **1b** (0.0906 mmol, 81 mg) in THF (5 mL) was added a solution of DIBAL-H in toluene (0.9 mL, 1.5 M) at 25 °C under an argon atmosphere. After the mixture was stirred at this temperature for 12 h, the resulting purple suspension was filtered through glass frits, and the solvent was removed from the filtrates under reduced pressure. The residue was washed with pentane and ether to yield 2-^{i}Bu$_2$AlCl$_2$ (69 mg, 73%). Single crystals of **3** were grown from THF/pentane at ambient temperature. ^{1}H NMR (benzene-d_6, rt): δ 2.73 (18H, s, NMe), 2.70 (2H, m, $AlCH_2CH$), 2.41 (24H, m, NCH_2), 1.57 (12H, d, J = 6.6 Hz, CH_3), 0.85 (4H, d, J = 6.6 Hz, $AlCH_2$), −24.0 (6H, s, μ-H) ppm. COSY (benzene-d_6, rt): 2.70/1.57, 0.85. ^{13}C{^{1}H} NMR (benzene-d_6, rt): δ 59.7 (NCH_2), 59.3 (NCH_3), 57.7 (AlCCH), 29.3 ($AlCCCH_3$), 27.4 ($AlCH_2$) ppm. HMQC (^{13}C/^{1}H, benzene-d_6, rt): δ 59.7/2.41; 59.3/2.73; 57.7/2.70; 29.3/1.57; 27.4/0.85. HMBC (^{13}C/^{1}H, benzene-d_6, rt): δ 57.7/1.57, 0.85; 29.3/2.70; 27.4/2.70. IR (KBr, cm^{-1}): ν 2852 (m), 1655 (s), 1578 (s), 1450 (s), 1052 (m), 1010 (s), 785 (s), 745 (s), 687 (s), 670 (s). Anal. Calcd for $C_{26}H_{66}Al_2Cl_2Fe_2N_6$: C, 44.65; H, 9.51; N, 12.02. Found: C, 44.91; H, 9.91; N, 11.45.

Synthesis of 3. To a suspension of **1b** (0.0906 mmol, 81 mg) in THF (5 mL) was added a solution of $NaAlH_2(OCH_2CH_2OMe)_2$ in toluene (3.6 M, 0.38 mL) at 25 °C under an argon atmosphere while the mixture immediately turned purple. After the mixture was stirred at this temperature for 12 h, the resulting purple suspension was filtered through glass frits, and the solvent was removed from the filtrates under reduced pressure. The residue was washed with toluene and ether to afford **3** (91 mg, 76%). Single crystals of **3** were grown from THF/ether at ambient temperature. ^{1}H NMR (THF-d_8, rt): δ 3.92 (4H, t, J = 5.6 Hz, OCH_2), 3.79 (4H, t, J = 5.6 Hz, OCH_2), 3.67 (4H, t, J = 5.6 Hz, OCH_2), 3.43 (4H, t, J = 5.6 Hz, OCH_2), 3.41 (6H, s,

dx.doi.org/10.1021/ic500195q | Inorg. Chem. 2014, 53, 5100−5108

OCH_3), 3.33 (6H, s, OCH_3), 3.06 (12H, m, NCH_2), 2.95 (18H, s, NMe), 2.93 (12H, m, NCH_2), −25.6 (6H, s, μ-H) ppm. COSY (THF-d_6, rt): 3.92/3.67; 3.79/3.43; 3.06/2.93. $^{13}C\{^1H\}$ NMR (THF-d_8, rt): δ 78.1 (OCH_2), 74.4 (OCH_2), 61.0 (OCH_2), 60.3 (NCH_2), 60.0 (OCH_2), 59.6 (NCH_3), 58.7 (OCH_3), 58.3 (OCH_3) ppm. HMQC ($^{13}C/^1H$, THF-d_8, rt): δ 78.1/3.43; 74.4/3.67; 61.0/3.79; 60.3/3.06, 2.93; 60.0/3.92; 59.6/2.95; 58.7/3.33; 58.3/3.41. HMBC ($^{13}C/^1H$, THF-d_8, rt): δ 78.1/3.79; 74.4/3.92; 61.0/3.43; 60.3/3.06, 2.93; 60.0/3.67. IR (KBr, cm^{-1}): ν 2851 (s), 1655 (s), 1648 (s), 1638 (s), 1458 (s), 1119 (s), 1086 (s), 1014 (s), 835 (s), 763 (s), 603 (m). Anal. Calcd for $C_{30}H_{76}Al_2ClFe_2N_6NaO_8$: C, 41.27; H, 8.77; N, 9.63. Found: C, 41.70; H, 9.81; N, 9.64.

Synthesis of 4. In the glovebox, to a suspension of **1b** (0.101 mmol, 90 mg) in THF (7 mL) was added $\{Li(OEt_2)_2\}\{Al(OC_6H_3$-2,6-$^tBu_2)_2\}(\mu$-$H)_2$ (1.56 mmol, 930 mg) at room temperature. The mixture was stirred for 15 h while the system was closed. Then, insoluble byproduct was filtered and solvent was evaporated from the filtrate. Washing the residue with ether and a small amount of toluene followed by dryness *in vacuo* gave **4** as a red-purple solid (190 mg, 94%). Single crystals were obtained from a THF solution by slow diffusion of ether. ^1H NMR (THF-d_8, rt): δ 6.99 (4H, d, J = 7.6 Hz, Ar−H, *meta*), 6.42 (2H, t, J = 7.6 Hz, Ar−H, *para*), 2.69−2.59 (12H, m, NCH_2), 2.37 (9H, s, NMe), 1.59 (36H, s, ^tBu), −25.20 (3H, s, μ-H) ppm. COSY (THF-d_8, rt): 6.99/6.42. $^{13}C\{^1H\}$ NMR (THF-d_8, rt): δ 160.2 (Ar, *ipso*), 139.9 (Ar, *ortho*), 124.9 (Ar, *meta*), 116.2 (Ar, *para*), 60.1 (NCH_2), 58.7 (NCH_3), 36.3 (CMe_3), 33.3 (CMe_3) ppm. HMQC ($^{13}C/^1H$, THF-d_8, rt): δ 124.9/6.99; 116.2/6.42; 60.1/2.69−2.59; 58.7/2.37; 33.3/1.59. HMBC ($^{13}C/^1H$, THF-d_8, rt): δ 160.2/6.99; 139.9/6.42; 36.3/6.99, 1.59. IR (KBr, cm^{-1}): ν 2950 (s), 1719 (m), 1638 (m), 1408 (s), 1245 (s), 1013 (s), 895 (s), 866 (s), 750 (s), 677 (s). Anal. Calcd for $C_{41}H_{74}AlFeN_3O_3$: C, 66.56; H, 10.08; N, 5.68. Found: C, 66.70; H, 10.65; N, 5.77.

Calculation Methods. All geometry optimizations, vibrational frequencies, and energy calculations were carried out using the density functional theory (DFT)[22] at the B3LYP level[23,24] with a mixed basis set in the Gaussian03 program.[25] The mixed basis set contained 3-21G[26] for the carbons and hydrogens of Me_3tacn and aryloxide ligands and the oxygens of aryloxide ligands, 6-31G for nitrogens of Me_3tacn and the hydrogens of the bridging ligands, and 6-31+G(d,p)[27−31] for irons and aluminum. Wiberg bond indexes[32,33] were calculated using natural bond orbital (NBO) analysis.[34]

■ ASSOCIATED CONTENT

Ⓢ Supporting Information

X-ray crystallographic data for **2**−**4** in cif format. Cartesian coordinates of **2** and **4** from the computation. Diagrams of molecular orbitals of the singlet states of **2** and **4**. This material is available free of charge via the Internet at http://pubs.acs.org.

■ AUTHOR INFORMATION

Corresponding Author

*E-mail: hiroharu@o.cc.titech.ac.jp.

Notes

The authors declare no competing financial interest.

■ ACKNOWLEDGMENTS

The Japan Society for the Promotion of Science (a Grant-in-Aid for Scientific Research (S), grant no. 18105002) is gratefully acknowledged for funding this research. We also thank Dr. Hiroyasu Sato from Rigaku Corp. for assistance with X-ray structure determination.

■ REFERENCES

(1) (a) Cowan, J. A. *Inorganic Biochemistry: An Introduction*, 2nd ed.; Wiley-VCH: New York, 1997. (b) Kessissoglou, D. P. *Bioinorganic Chemistry: An Inorganic Perspective of Life*; NATO ASI Series C, Vol. *459*; Kluwer Academic Publishers: Dordrecht, 1995.

(2) Wieghardt, K.; Pohl, K.; Gebert, W. *Angew. Chem., Int. Ed. Engl.* **1983**, *22*, 727.

(3) Armstrong, W. H.; Spool, A.; Papaefthymiou, G. C.; Frankel, R. B.; Lippard, S. J. *J. Am. Chem. Soc.* **1984**, *106*, 3653.

(4) Hanke, D.; Wieghardt, K.; Nuber, B.; Lu, R.-S.; McMullan, R. K.; Koetzle, T. F.; Bau, R. *Inorg. Chem.* **1993**, *32*, 4300.

(5) Namura, K.; Kakuta, S.; Suzuki, H. *Organometallics* **2010**, *29*, 4305.

(6) Paneque, M.; Poveda, M. L.; Salazar, V.; Taboada, S.; Carmona, E.; Gutiérrez-Puebla, E.; Monge, A.; Ruiz, C. *Organometallics* **1999**, *18*, 139.

(7) (a) Shima, T.; Namura, K.; Kameo, H.; Kakuta, S.; Suzuki, H. *Organometallics* **2010**, *29*, 337. (b) Namura, K.; Ohashi, M.; Suzuki, H. *Organometallics* **2012**, *31*, 5979.

(8) We assign the cation structure of **2′**-BPh_4 to $[\{(Me_3tacn)Fe\}(\mu$-$H)_3Al(OBu)_2]_2M(solvent)_n$ (M = Li or Na). The X-ray structure was not completely solved because several carbon atoms of BuO groups on the aluminum atoms, which should result from ring-opening of THF, could hardly be located from the X-ray diffraction data.

(9) (a) Weiss, J.; Stetzkamp, D.; Nuber, B.; Fischer, R. A.; Boehme, C.; Frenking, G. *Angew. Chem., Int. Ed. Engl.* **1997**, *36*, 70. (b) Steinke, T.; Cokoja, M.; Gemel, C.; Kempter, A.; Krapp, A.; Frenking, G.; Zenneck, U.; Fischer, R. A. *Angew. Chem., Int. Ed.* **2005**, *44*, 2943. (c) Buchin, B.; Gemel, C.; Kempter, A.; Cadenbach, T.; Fischer, R. A. *Inorg. Chim. Acta* **2006**, *359*, 4833.

(10) (a) Fischer, R. A.; Priermeier, T. *Organometallics* **1994**, *13*, 4306. (b) Braunschweig, H.; Müller, J.; Ganter, B. *Inorg. Chem.* **1996**, *35*, 7443. (c) Anand, B. N.; Krossing, I.; Nöth, H. *Inorg. Chem.* **1997**, *36*, 1979. (d) Jones, C.; Aldridge, S.; Gans-Eichler, T.; Stasch, A. *Dalton Trans.* **2006**, *1*, 5357. (e) Riddlestone, I. M.; Edmonds, S.; Kaufman, P. A.; Urbano, J.; Bates, J. I.; Kelly, M. J.; Thompson, A. L.; Taylor, R.; Aldridge, S. *J. Am. Chem. Soc.* **2012**, *134*, 2551. (f) Burlitch, J. M.; Leonowicz, M. E.; Petersen, R. B.; Hughes, R. E. *Inorg. Chem.* **1979**, *18*, 1097.

(11) Akitt, J. W. In *Aluminum, Gallium, Indium, Thallium*; Mason, J., Ed.; Multinuclear NMR; Plenum Press: New York, 1987; Chapter 9.

(12) (a) Skupiñsksi, W. A.; Huffman, J. C.; Bruno, J. W.; Caulton, K. G. *J. Am. Chem. Soc.* **1984**, *106*, 8128. (b) Barron, A. R.; Willkinson, G.; Motevalli, M.; Hursthouse, M. B. *J. Chem. Soc., Dalton Trans.* **1987**, 837. (c) Conroy, K. D.; Piers, W. E.; Parvez, M. *Organometallics* **2009**, *28*, 6228.

(13) (a) Cotton, F. A.; Murillo, L. A.; Walton, R. A. *Multiple Bonds Between Metal Atoms*, 3rd ed.; Springer: New York, 2005. (b) Pauling, L. *The Nature of the Chemical Bond*, 3rd ed.; Cornell University Press: Ithaca, 1960.

(14) (a) Hillier, A. C.; Jacobsen, H.; Gusev, D.; Schmalle, H. W.; Berke, H. *Inorg. Chem.* **2001**, *40*, 6334. (b) Guilera, G.; McGrady, G. S.; Steed, J. W.; Kaltsoyannis, N. *New J. Chem.* **2004**, *28*, 444.

(15) Moreland, A. C.; Rauchfuss, T. B. *Inorg. Chem.* **2000**, *39*, 3029.

(16) Hamilton, D. G.; Crabtree, R. H. *J. Am. Chem. Soc.* **1988**, *110*, 4126.

(17) Nöth, H.; Schlegel, A.; Knizek, J.; Krossing, I.; Ponikwar, W.; Seifert, T. *Chem.—Eur. J.* **1998**, *4*, 2191.

(18) (a) Lever, A. B. P. *Inorganic Electronic Spectroscopy*, 2nd ed.; Elsevier: Amsterdam, 1984. (b) Wieghardt, K.; Schmidt, W.; Herrmann, W.; Küppers, H.-J. *Inorg. Chem.* **1983**, *22*, 2953. (c) Bossek, U.; Nühlen, D.; Bill, E.; Glaser, T.; Krebs, C.; Weyhermüller, T.; Wieghardt, K.; Lengen, M.; Trautwein, A. X. *Inorg. Chem.* **1997**, *36*, 2834. (d) Blakesley, D. W.; Payne, S. C.; Hagen, K. S. *Inorg. Chem.* **2000**, *39*, 1979. (e) Bölrzel, H.; Comba, P.; Pritzkow, H.; Sickmüller, A. F. *Inorg. Chem.* **1998**, *37*, 3853. (f) Martin, L. L.; Martin, R. L.; Sargeson, A. M. *Polyhedron* **1994**, *13*, 1969.

(19) Diebold, A.; Elbouadili, A.; Hagen, K. S. *Inorg. Chem.* **2000**, *39*, 3915.

(20) (a) Ghilardi, C. A.; Innocenti, P.; Midollini, S.; Orlandini, A. *J. Organomet. Chem.* **1982**, *231*, C78. (b) Ghilardi, C. A.; Innocenti, P.; Midollini, S.; Orlandini, A. *J. Chem. Soc., Dalton Trans.* **1985**, 605. (c) Schaeffer, G. W.; Roscoe, J. S.; Stewart, A. C. *J. Am. Chem. Soc.* **1956**, *78*, 729. (d) Monnier, G. *Ann. Chim. (Paris)* **1957**, *2*, 14.

(e) Mehn, M. P.; Brown, S. D.; Paine, T. K.; Brennessel, W. W.; Cramer, C. J.; Peters, J. C.; Que, L., Jr. *Dalton Trans.* **2006**, 1347. (f) Gilbert, S.; Knorr, M.; Mock, S.; Schubert, U. *J. Organomet. Chem.* **1994**, *480*, 241. (g) Thomas, C. M.; Peters, J. C. *Angew. Chem., Int. Ed.* **2006**, *45*, 776.

(21) Sheldrick, G. M. *SHELX-97*; University of Göttingen, 1997.

(22) Becke, A. D. *J. Chem. Phys.* **1993**, *98*, 5648.

(23) Becke, A. D. *Phys. Rev.* **1988**, *A38*, 3098.

(24) Lee, C.; Yang, W.; Parr, R. G. *Phys. Rev.* **1988**, *B37*, 785.

(25) Frisch, M. J.; Trucks, G. W.; Schlegel, H. B.; Scuseria, G. E.; Robb, M. A.; Cheeseman, J. R.; Montgomery, J. A., Jr.; Vreven, T.; Kudin, K. N.; Burant, J. C.; Millam, J. M.; Iyengar, S. S.; Tomasi, J.; Barone, V.; Mennucci, B.; Cossi, M.; Scalmani, G.; Rega, N.; Petersson, G. A.; Nakatsuji, H.; Hada, M.; Ehara, M.; Toyota, K.; Fukuda, R.; Hasegawa, J.; Ishida, M.; Nakajima, T.; Honda, Y.; Kitao, O.; Nakai, H.; Klene, M.; Li, X.; Knox, J. E.; Hratchian, H. P.; Cross, J. B.; Bakken, V.; Adamo, C.; Jaramillo, J.; Gomperts, R.; Stratmann, R. E.; Yazyev, O.; Austin, A. J.; Cammi, R.; Pomelli, C.; Ochterski, J. W.; Ayala, P. Y.; Morokuma, K.; Voth, G. A.; Salvador, P.; Dannenberg, J. J.; Zakrzewski, V. G.; Dapprich, S.; Daniels, A. D.; Strain, M. C.; Farkas, O.; Malick, D. K.; Rabuck, A. D.; Raghavachari, K.; Foresman, J. B.; Ortiz, J. V.; Cui, Q.; Baboul, A. G.; Clifford, S.; Cioslowski, J.; Stefanov, B. B.; Liu, G.; Liashenko, A.; Piskorz, P.; Komaromi, I.; Martin, R. L.; Fox, D. J.; Keith, T.; Al-Laham, M. A.; Peng, C. Y.; Nanayakkara, A.; Challacombe, M.; Gill, P. M. W.; Johnson, B.; Chen, W.; Wong, M. W. ; Gonzalez, C.; Pople, J. A.*Gaussian 03*, Revision D.02; Gaussian, Inc.: Wallingford, CT, 2004.

(26) Binkley, J. S.; Pople, J. A.; Hehre, W. J. *J. Am. Chem. Soc.* **1980**, *102*, 939.

(27) Hehre, W. J.; Ditchfield, R.; Pople, J. A. *J. Chem. Phys.* **1972**, *56*, 2257.

(28) Francl, M. M.; Petro, W. J.; Hehre, W. J.; Binkley, J. S.; Gordon, M. S.; DeFrees, D. J.; Pople, J. A. *J. Chem. Phys.* **1982**, *77*, 3654.

(29) Rassolov, V.; Pople, J. A.; Ratner, M.; Windus, T. L. *J. Chem. Phys.* **198**, *109*, 1223.

(30) Clark, T.; Chandrasekhar, J.; Spitznagel, G. W.; Schleyer, P. v. R. *J. Comput. Chem.* **1983**, *4*, 294.

(31) Frisch, M. J.; Pople, J. A.; Binkley, J. S. *J. Chem. Phys.* **1984**, *80*, 3265.

(32) Wiberg, K. B. *Tetrahedron* **1968**, *24*, 1083.

(33) Mayer, I. *Theor. Chim. Acta* **1985**, *67*, 315.

(34) Glendening, E. D.; Badenhoop, J. K.; Reed, A. E.; Carpenter, J. E.; Bohmann, J. A.; Morales, C. M.; Weinhold, F. *NBO* 5.G; Theoretical Chemistry Institute, University of Wisconsin: Madison, WI, 2001.